This article was downloaded by:
On: *14 January 2011*
Access details: *Access Details: Free Access*
Publisher *Taylor & Francis*
Informa Ltd Registered in England and Wales Registered Number: 1072954 Registered office: Mortimer House, 37-41 Mortimer Street, London W1T 3JH, UK

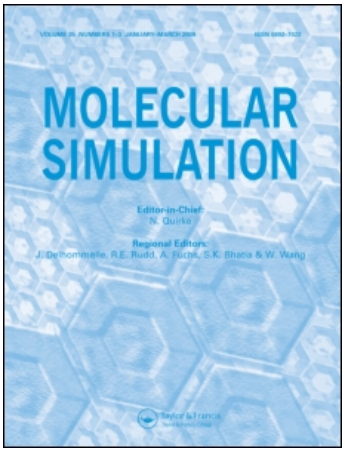

Molecular Simulation
Publication details, including instructions for authors and subscription information:
http://www.informaworld.com/smpp/title~content=t713644482

Investigation of the Air Separation Properties of Zeolites Types A, X and Y by Monte Carlo Simulations

K. Watanabe[a]; N. Austin[a]; M. R. Stapleton[a]
[a] Molecular Simulations Ltd., Cambridge, UK

To cite this Article Watanabe, K. , Austin, N. and Stapleton, M. R.(1995) 'Investigation of the Air Separation Properties of Zeolites Types A, X and Y by Monte Carlo Simulations', Molecular Simulation, 15: 4, 197 — 221
To link to this Article: DOI: 10.1080/08927029508022335
URL: http://dx.doi.org/10.1080/08927029508022335

PLEASE SCROLL DOWN FOR ARTICLE

Full terms and conditions of use: http://www.informaworld.com/terms-and-conditions-of-access.pdf

This article may be used for research, teaching and private study purposes. Any substantial or systematic reproduction, re-distribution, re-selling, loan or sub-licensing, systematic supply or distribution in any form to anyone is expressly forbidden.

The publisher does not give any warranty express or implied or make any representation that the contents will be complete or accurate or up to date. The accuracy of any instructions, formulae and drug doses should be independently verified with primary sources. The publisher shall not be liable for any loss, actions, claims, proceedings, demand or costs or damages whatsoever or howsoever caused arising directly or indirectly in connection with or arising out of the use of this material.

Molecular Simulation, 1995, Vol. 15, pp. 197–221
Reprints available directly from the publisher
Photocopying permitted by license only

© 1995 OPA (Overseas Publishers Association)
Amsterdam B.V. Published under license by
Gordon and Breach Science Publishers SA
Printed in Malaysia

INVESTIGATION OF THE AIR SEPARATION PROPERTIES OF ZEOLITES TYPES A, X AND Y BY MONTE CARLO SIMULATIONS

K. WATANABE, N. AUSTIN and M. R. STAPLETON

Molecular Simulations Ltd., 240/250 The Quorum, Barnwell Road, Cambridge, CB5 8RE, UK

(Received December 1994, accepted March 1995)

The air separation properties of zeolite types *A*, *X*, and *Y* have been studied using grand canonical Monte Carlo simulations of nitrogen, oxygen, and argon adsorbed in these zeolite lattices. Nitrogen is adsorbed preferentially due to the quadrupole-ion electrostatic interactions with the extra framework cations. The localization of adsorption sites for nitrogen near cations and the more diffuse distributions of oxygen and argon within zeolite cavities are clearly illustrated. Predicted nitrogen/oxygen selectivity for 5A from simulations is in good agreement with that determined experimentally. The effect of the calcium-sodium ion exchange on the predicted nitrogen/oxygen selectivity is examined, and is shown to be sensitive to the magnitude of the charges assigned to the extra framework cations.

KEY WORDS: Zeolites, Gas separation, Monte Carlo simulation

Downloaded At: 19:23 14 January 2011

INTRODUCTION

Zeolites are used extensively in the gas separation industry. The unique capability of zeolites to selectively adsorb different molecular species arises from the varied nature of the interactions with different types of molecules. The capacity of some zeolites to selectively adsorb nitrogen over oxygen and argon provides a method for effective separation of nitrogen from air. The nitrogen selectivity is a result of the interaction of the quadrupole moment of nitrogen molecules with the electric field within zeolite lattices.

This study modelled the selective adsorption of nitrogen versus oxygen in types *A*, *X*, and *Y* zeolites using grand canonical Monte Carlo simulations. The effects of the type and numbers of extra framework cations and their accessibility to the adsorbed molecules on the efficiency of the zeolites for air separation were examined. The simulation method allows the determination of the equilibrium uptake of adsorbate molecules by a zeolite lattice at specified pressure, composition, and temperature, leading to determination of adsorption isotherms for single and multi-component gases. Further, molecular configurations generated during the simulations were examined for the presence of preferred adsorption sites within the zeolite lattices.

Several studies utilizing grand canonical Monte Carlo simulations of adsorption in zeolites have been reported [1]. In particular, adsorption of air was studied for the 5A

zeolite by Razmus and Hall [1d]. This work successfully reproduced experimental single-component adsorption isotherms for argon, oxygen and nitrogen, but the simulations could not quantitatively predict experimental data for mixture adsorption. As a possible source of the failure the authors speculated that the electrostatic interaction between adsorbates and zeolite may have been incorrectly modelled due to errors in the estimation of the charge distribution within the zeolite. In the present work, the effect of the charge assignment on the predicted nitrogen/oxygen selectivity is examined in detail for zeolites with type A and faujasite frameworks.

The paper is arranged as follows. The details of the potential model and the computational procedures are described in section 2. The adjustable parameters for the potential model are determined by fitting to experimental Henry's constants for silicalite and 5A zeolite in section 3. Results of the simulations for the nitrogen/oxygen selectivities of zeolite types A, X, and Y are presented in section 4, which includes a discussion of the effect of the sodium-calcium ion exchange on the nitrogen/oxygen selectivity of these zeolites. Section 5 provides a summary of the conclusions for this study.

Downloaded At: 19:23 14 January 2011

2. THE POTENTIAL MODEL AND COMPUTATIONAL PROCEDURES

The total potential energy U of the zeolite lattice and adsorbed molecules is written as the sum of the interaction energy between the adsorbate and the zeolite, U_{AZ}, and that between the adsorbates, U_{AA},

$$U = U_{AZ} + U_{AA} \tag{1}$$

U_{AZ} and U_{AA} are both written as sums of pairwise additive potentials u_{ij} of the form,

$$u_{ij} = 4\varepsilon_{ij}[(\sigma_{ij}/r_{ij})^{12} - (\sigma_{ij}/r_{ij})^{6}] + (q_i q_j / r_{ij}) \tag{2}$$

where the first term is the Lennard-Jones (LJ) 12–6 potential and the second term is the Coulomb interaction potential between point charges q_i and q_j of sites i and j separated by distance r_{ij}.

The LJ potential for the adsorbate-zeolite interactions and both the LJ and Coulombic terms of the adsorbate-adsorbate interactions were calculated using the minimum image convention [2] with potential cut-off distance of 12 Å. The Coulombic term for the adsorbate-zeolite interactions was evaluated using the Ewald summation method [3].

Monte Carlo simulations in the grand canonical ensemble were carried out using the standard procedure [2] involving creation and destruction of molecules which interact with the potential field generated by the atoms comprising the zeolite lattice, which is assumed rigid. Molecular creation attempts are made at points chosen randomly within the zeolite lattice (simulation box) with volume V. A creation attempt is accepted with a probability,

$$P_C = \min [1, (V/(N+1)\Lambda^3)\exp(-\Delta U + \mu/k_B T)] \tag{3}$$

where N is the number of molecules in the simulation box before the molecular creation attempt, ΔU is the change in the total potential energy accompanying the creation

attempt, μ is the chemical potential and Λ is the thermal de Broglie wavelength. For molecular destruction attempts a molecule is selected at random from N existing molecules and the attempt to destroy the molecule is accepted with a probability,

$$P_d = \min [1, (N\Lambda^3/V)\exp(-\Delta U - \mu/k_BT)] \tag{4}$$

In the grand canonical ensemble the chemical potential of adsorbed molecules equals the chemical potential of the bulk phase, which can be written [4] as a function of temperature and fugacity, f,

$$\mu = k_BT\ln(f\Lambda^3/k_BT), \tag{5}$$

which, substituted into equations (3) and (4) gives,

$$P_C = \min [1, (fV/(N+1)k_BT)\exp(-\Delta U/k_BT)] \tag{6}$$

and

$$P_d = \min [1, (Nk_BT/fV)\exp(-\Delta U/k_BT)] \tag{7}$$

At the low pressure conditions considered here, bulk gases can be assumed to obey the ideal gas law and fugacity can be replaced by gas pressure, P, or partial pressures, P_i, in the case of multi-component gases. In addition to the creation and destruction attempts, which were attempted with equal probability, displacement and rotation of molecules were allowed. Attempts to either displace or rotate a molecule were accepted with a probability P given by,

$$P = \min [1, \exp(-\Delta U/k_BT)] \tag{8}$$

where ΔU is the change in the potential energy accompanying the displacement or rotation attempt.

For the present simulations, calculation of ΔU was preceded by a check for overlapping interaction sites. If a pair of interaction sites were closer than a pre-assigned distance, the sites were considered to be overlapping. The distance used for the criterion of overlap was set equal to half the sum of the van der Waals radii for the two sites. Any attempt to create, displace, or rotate a molecule accompanying an overlapping of sites was not accepted. If the sites were not overlapping, ΔU was evaluated to determine whether to accept the attempt or not in accordance with the appropriate acceptance probabilites. This procedure amounts to imposing impenetrable hard cores to interaction sites, and therefore the non-Coulombic part of the pairwise interaction potential is the LJ potential supplemented by the hard sphere potential.

For zeolite lattices, hard cores were assigned to silicon, aluminium oxygen, and the extra framework cations. In addition to these zeolite atoms, we placed hard cores at the centres of sodalite cages which are present in the type A and faujasite structures. This effectively blocked the sodalite cages from adsorbing molecules, which may otherwise have occured since the creation attempts were made randomly at any point within the simulation box without any biasing. For the adsorbate molecules considered in the present work, the interior of a sodalite cage is expected to be inaccessible via diffusion from the main channels due to the narrowness of the 4T and 6T ring apertures of the sodalite cage. In the present simulations the centres of the sodalite cages were thus

Downloaded At: 19:23 14 January 2011

treated as interaction sites with hard cores, but are otherwise non-interacting with adsorbate molecules.

3. INTERMOLECULAR POTENTIAL PARAMETERS

3.1 Adsorbate–Adsorbate Interactions

Three types of adsorbate molecules are considered in this work; argon, oxygen, and nitrogen. Argon is represented by an LJ interaction site, while oxygen and nitrogen are represented by a three-site model. In this latter model, the two outer sites (of the three colinear sites) are separated by a distance l, and are LJ interaction sites as well as the location of point charges of equal magnitude q; the third site is located at the midpoint of the outer sites and has a point charge $-2q$ ensuring molecular charge neutrality. For the adsorbate-adsorbate type of interactions, literature potentials were adopted. The LJ potential parameters for argon, ε_{Ar} and σ_{Ar}, were given values 0.2381 kcal/mol and 3.405 Å [5], respectively. For oxygen, we chose $q = -0.112\,|e|$ and $l = 1.21$ Å, which results in the experimental [6] quadrupole moment -1.3×10^{-40} Cm^2 and the LJ parameters $\sigma_O = 3.05$Å and $\varepsilon_O = 0.108$ kcal/mol were used [7]. For nitrogen the potential model X1, developed by Murthy *et al.* [8] with $l = 1.098$Å, $q = -0.40484\,|e|$, $\sigma_N = 3.318$Å, and $\varepsilon_N = 0.07233$ kcal/mol was used. This model for nitrogen gives a quadrupole moment of -3.91×10^{-40} Cm^2.

3.2 Adsorbate–Zeolite Interactions

3.2.1 Method The adsorbate–zeolite interaction potentials were determined based on the experimentally determined Henry's constant, K_H, defined as,

$$K_H = \lim(P \to 0)(N/P) \tag{9}$$

where N is the number of adsorbed molecules at pressure P. The potentials were derived by introducing parameters into the expression for U_{AZ} and adjusting them to attain a fit between the calculated K_H and the experimentally determined values. K_H was calculated from the expression,

$$K_H(T) = [1/4\pi k_B T] \int_0^{2\pi} d\varphi \int_0^{\pi} \sin\theta\, d\theta \int_V \int \exp\,[-U_{AZ}(\mathbf{r}, \theta, \varphi)]\mathbf{dr} \tag{10}$$

where the spherical polar coordinates, θ and φ, specify molecular orientation, and the position vector, r, specifies the location of the molecule within the volume, V, of the zeolite lattice. Equation (10) was evaluated numerically using the Monte Carlo intergration method [9].

Interaction sites placed on the zeolitic oxygen, silicon and aluminium and on the extra framework cations served as both the LJ interaction sites and the locations of point charges. A charge of $-1.0\,|e|$ was assigned to the oxygen atoms. This choice was based on the estimates obtained by Van Genechten and Mortier [10] for the charge

Downloaded At: 19:23 14 January 2011

distributions in various zeolite framework types using the electronegativity equalization method [11] which resulted in partial charges on oxygen in the vicinity of $-1.0|e|$. In previous simulation studies, including [1d], charges corresponding to full ionization have typically been assigned to the extra framework cations. In the present work the cations are in some cases assumed partially ionized and their charges treated as adjustable parameters. The reasons for this preference are discussed below. The charges on silicon and aluminium are assumed to be equal and are determined by the requirement for the electrical neutrality of the zeolite lattices.

Following the empirical approach used by Razmus and Hall [1d], the attractive part of the LJ potential was written as $-\beta_i\alpha_i\alpha_j/r_{ij}^6$ where β_i is an adjustable parameter characteristic of adsorbate i and α_i and α_j are the polarizabilities of atoms in the adsorbate molecules and in the zeolite lattice, respectively. The well depth of the LJ potential, ε_{ij}, can be written as,

$$\varepsilon_{ij} = \beta_i\alpha_i\alpha_j/4\sigma_{ij}^6 \tag{11}$$

with the LJ parameter σ_{ij} for the adsorbate-zeolite given by the mixing rule,

$$\sigma_{ij} = (\sigma_i + \sigma_j)/2 \tag{12}$$

The σ_i for the adsorbate molecules are those used for the adsorbate-adsorbate LJ potentials and the σ_i for the zeolite lattice are derived from van der Waals radii, R_i, of respective ions, which are related to σ_i by,

$$R_i = 2^{(1/6)}\sigma_i \tag{13}$$

The values for α_i and R_i used in the present work are taken from the literature and are given in Table 1. This leaves $\beta_i (i = \text{Ar, O, N})$ as the only adjustable parameter to determine the adsorbate-zeolite LJ potentials. Henry's constants were evaluated for the 5A and silicalite lattices. For the 5A zeolite, we used the coordinates given by Seff and Shoemaker [14] for a cubic unit cell with composition $Ca_4Na_4Al_{12}Si_{12}O_{48}$ and cell dimension 12.29 Å. A cubic lattice with side length 24.58 Å which contains 8 unit cells was used as a simulation box. Similarly, a silicalite lattice was constructed by $2 \times 2 \times 2$

Table 1 Values of polarizabilities, α, and van der Waals radii, R, used in the determination of the adsorbate-zeolite LJ potentials

Atom type	α(Å^3)	R(Å)
Ar	1.64[a]	3.822[c]
N	0.87[a]	3.724[c]
O	0.79[a]	3.424[c]
Oz	1.47[a]	3.040[a]
Si	0.04[b]	0.76[d]
Al	0.067[b]	1.14[d]
Na	0.18[a]	1.960[a]
Ca	0.471[a]	1.980[a]

[a] Adopted from the work of Razmus and Hall [1d].
[b] Reference [12].
[c] Values consistent with the adsorbate-adsorbate LJ potential patential parameter, σ, given in the text.
[d] Reference [13].

Downloaded At: 19:23 14 January 2011

replication of the unit cell with side lengths Lx = 20.002 Å, Ly = 19.899 Å, Lz = 13.383 Å using atomic coordinates determined by van Koningsveld [15]. In the implementation of the Monte Carlo integration technique to calculate K_H, the zeolite lattice was sampled randomly except for the volumes corresponding to an overlap of hard cores of the adsorbate atoms and zeolite interaction sites, which included those placed in the sodalite cages.

A survey of experimental Henry's constants for the gases in 5A revealed that there is poor agreement between the available experimental data [16, 17, 18, 19] with deviations by up to a factor of 1.8. This contributes to uncertainties in the generality of the resulting potential models obtained using the present semi-empirical approach. The potential parameter set presented in this paper is that obtained by a fit to Henry's constants for oxygen and nitrogen in 5A measured by Ruthven [16] at 298 K and those for argon, oxygen, and nitrogen in silicalite estimated from adsorption isotherms measured by Chaffee [20] at 298 K.

3.2.2 Parameterization Firstly, a fit to the experimental K_H [20] for silicalite at 298 K (0.77, 0.75, and 0.81 molecules/unit cell/bar for argon, oxygen, and nitrogen, respectively) was obtained by setting the adjustable parameters to $\beta_{Ar} =$ 295.8 kcal/mol, $\beta_O = 284.6$ kcal/mol, and $\beta_N = 287.8$ kcal/mol. Corresponding LJ parameters for the interactions of the gases with zeolite oxygens (Oz) with these choices for the β values are: $\varepsilon_{Ar-Oz} = 0.219$ kcal/mol, $\varepsilon_{O-Oz} = 0.145$ kcal/mol, and $\varepsilon_{N-Oz} =$ 0.123 kcal/mol. Using these ε_{ij} values and ε_{Ar}, ε_O, and ε_N given above and assuming the geometric combination rule given by,

$$\varepsilon_{ij} = (\varepsilon_i \varepsilon_j)^{0.5} \tag{14}$$

values can be determined for ε_{Oz}. The use of the above values for ε_{Ar-Oz}, ε_{O-Oz}, and ε_{N-Oz} results in the estimates for ε_{Oz} of 0.202, 0.195, 0.209 kcal/mol, respectively. The near constancy of the value for ε_{Oz} indicates the consistancy of the potential parameters with the geometric combination rule for ε. Figures 1, 2 and 3 show the adsorption isotherms calculated by grand canonical Monte Carlo simulations in comparison with experimental results [20] at T = 298 K and 333 K. The comparison is generally good. The best agreement with experiment is obtained at lower pressures, as expected, since the parameterization of the adsorbate-zeolite interactions was based on a comparison with experimental isotherms at the zero pressure limit. At higher pressures the simulation results tend to overestimate the experimental data. The cause of the disagreement at higher pressures may lie in the inadequate representation of the adsorbate-zeolite potential or of the adsorbate-adsorbate potentials which become more significant as pressure increases.

Secondly, a parameterization based on Ruthven's K_H values [16] for oxygen and nitrogen in 5A was carried out. This was initially attempted with charges on the cations set to the formal values; 1.0|e| for sodium and 2.0|e| for calcium. However, it was impossible to fit K_H for nitrogen by the adjustment of β_N alone, due to the dominant contribution from the Coulombic term. The same problem did not arise for oxygen as the-oxygen-zeolite interaction potential is dominated by the LJ term owing to the smaller quadrupole moment of the oxygen molecule. In order to circumvent the

Downloaded At: 19:23 14 January 2011

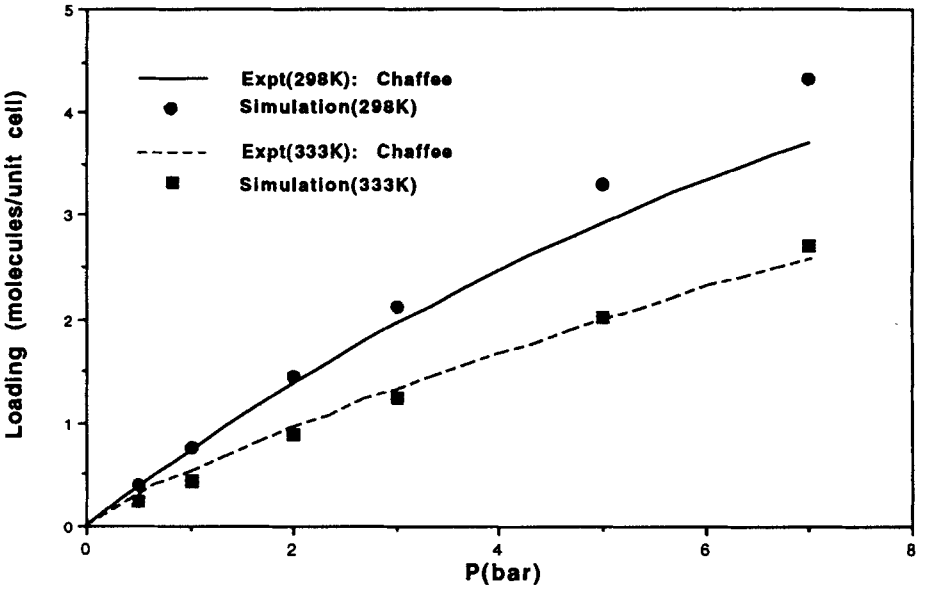

Figure 1 Adsorption isotherms for argon in silicalite at 298 K and 333 K. Simulation results are compared to experimental results of Chaffee [20].

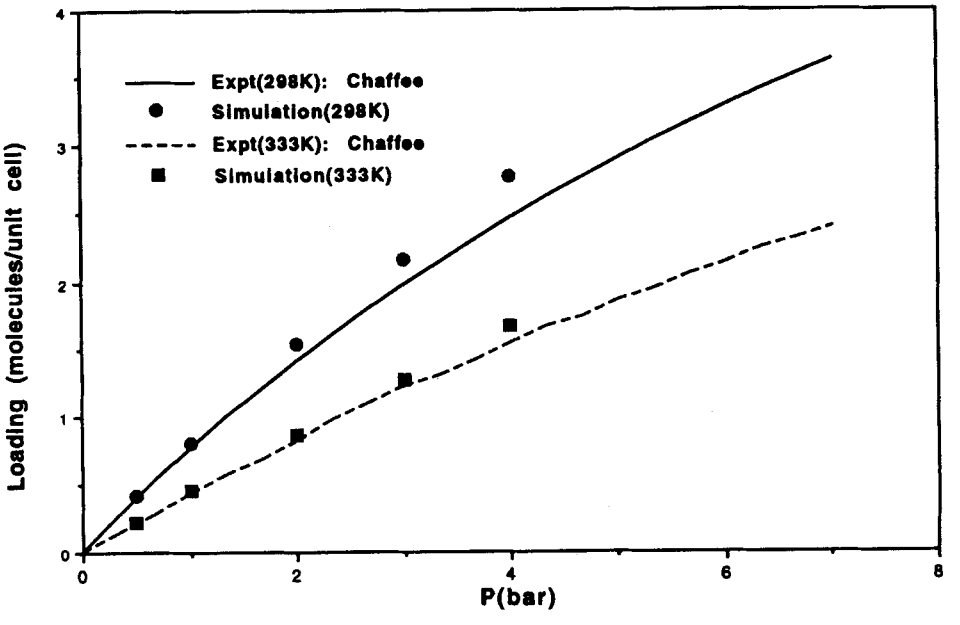

Figure 2 Adsorption isotherms for oxygen in silicalite at 298 K and 333 K. Simulation results are compared to experimental results of Chaffee [20].

Downloaded At: 19:23 14 January 2011

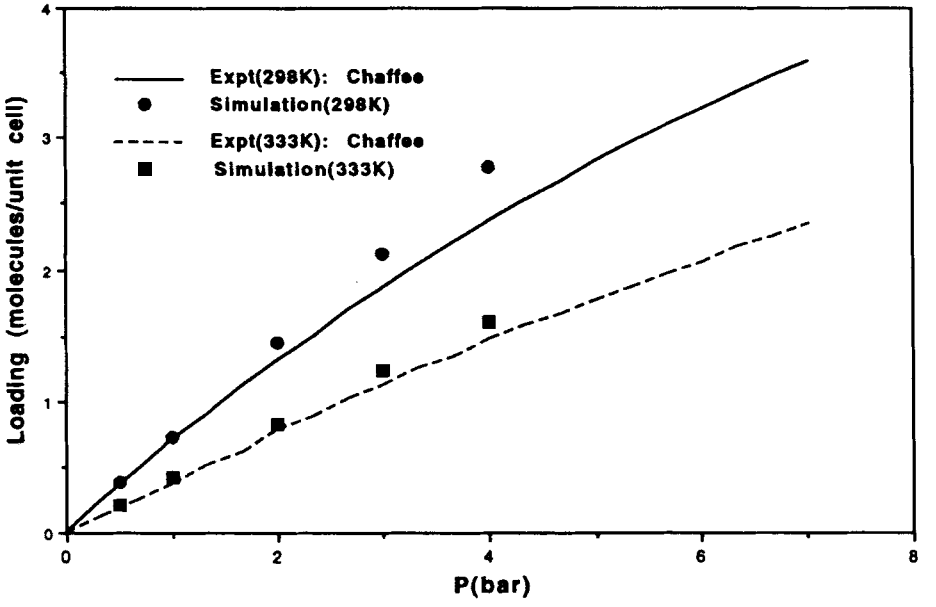

Figure 3 Adsorption isotherms for nitrogen in silicalite at 298 K and 333 K. Simulation results are compared to experimental results of Chaffee [20].

Downloaded At: 19:23 14 January 2011

difficulty for nitrogen, a reduction of charges on the cations was considered. Since a quantum mechanical study [21] had concluded that the charge transfer from the framework oxygen atoms to sodium ions is negligible, only the charge on the calcium ion was allowed to decrease, and thus was treated as an additional adjustable parameter as mentioned earlier. Therefore, the three parameters β_O, β_N, and q_{Ca} were adjusted so that the calculated k_H values for oxygen and nitrogen in 5A at 298 K were consistent with the experimental values of Ruthven [16]. These adjustments incorporated a constraint such that the ratio of the parameters β_O and β_N is constant at a value determined from the fit to the silicalite data. Further, by extending the assumption of the constancy of the ratios of the β values to those involving β_{Ar}, a value of β_{Ar} appropriate for 5A was obtained. This constraint implies that the description of the adsorbate-zeolite interactions in silicalite and in 5A are equivalent in terms of relative dispersion attractive interactions of different gas molecules with a zeolite lattice. The following parameters were obtained for 5A: $\beta_{Ar} = 380.7$ kcal/mol, $\beta_O = 366.3$ kcal/mol, $\beta_N = 370.4$ kcal/mol, and $q_{Ca} = 1.61$ |e|. Corresponding LJ parameters with these choices for β values are $\varepsilon_{Ar-Oz} = 0.282$ kcal/mol, $\varepsilon_{O-Oz} = 0.187$ kcal/mol, and, $\varepsilon_{N-Oz} = 0.158$ kcal/mol. Using the geometric combination rule for ε, ε_{Oz} is calculated to be 0.334, 0.332, and 0.347 kcal/mol from the values for ε_{Ar-Oz}, ε_{O-Oz}, and ε_{N-Oz}, respectively. For the two types of zeolite lattices considered here, significantly different estimates for ε_{Oz} emerged; 0.202 kcal/mol for silicalite and 0.334 kcal/mol for 5A. Recently, Pellenq and Nicholson [22] reported on the values for the polarizabilities of framework atoms in silicates and aluminosilicates determined from Auger electron

spectroscopy data. It was found that in the case of zeolite compounds the polarizability for an oxygen is sensitive to the ratio of silicon to aluminium and the nature of extra framework cations. The present parameterization implies a higher dispersion interaction of adsorbates with 5A framework oxygen than with silicalite oxygen. This is consistent with the higher values obtained for averaged oxygen polarizabilities for high aluminium-content zeolites (NaA, NaX, NaY) as compared to zeolites with lower aluminium content [22].

Table 2 presents the final set of parameters, ε_i and σ_i, determined for the zeolite interaction sites. We have assigned the ε_{O_z} values determined for silicalite and 5A, respectively, to oxygen connected to silicon only, Oz(Si-O-Si), and to oxygen connected to an aluminium, Oz(Al-O-Si). This assignment is a simplistic one which ignores the dependence [22] of the oxygen polarizability on the type of extra framework cation. Nevertheless these parameters are treated as transferable in the work presented below, i.e. calculations aimed at studying the nitrogen/oxygen selectivities of zeolite types *A*, *X*, and *Y* with sodium and calcium as counterions. The selectivity arises mainly from the difference in the Coulombic interactions of nitrogen and oxygen with the zeolite lattice, and the dispersion potential is of lesser importance for this relative quantity than it would be for absolute loading.

Downloaded At: 19:23 14 January 2011

4. RESULTS AND DISCUSSIONS

All the Monte Carlo simulations and analyses reported in this paper were performed using the Cerius^2 computational chemistry software [23].

4.1 Zeolite Type A

4.1.1 Comparison with experimental data Grand canonical Monte Carlo simulations were carried out for both pure and multicomponent gases of argon, oxygen, and nitrogen adsorbed in zeolite 5A. The results were compared with available experimental adsorption isotherms. Figures 4, 5 and 6 compare simulation results for the pure gases obtained at 297 K and 233 K with experimental isotherms measured by Miller [19]. As can be seen, agreement with experiment is less satisfactory for argon compared to that for nitrogen and oxygen. Simulation results for the adsorption of argon in 5A is

Table 2 Values of the LJ potential parameters for the zeolite interaction sites

Atom type	σ_i(Å)	ε_i(kcal/mol)
Oz(Si-O-Si)	2.708	0.202
Oz(Si-O-Al)	2.708	0.334
Si	0.677	0.037
Al	1.016	0.038
Na	1.746	0.041
Ca	1.764	0.272

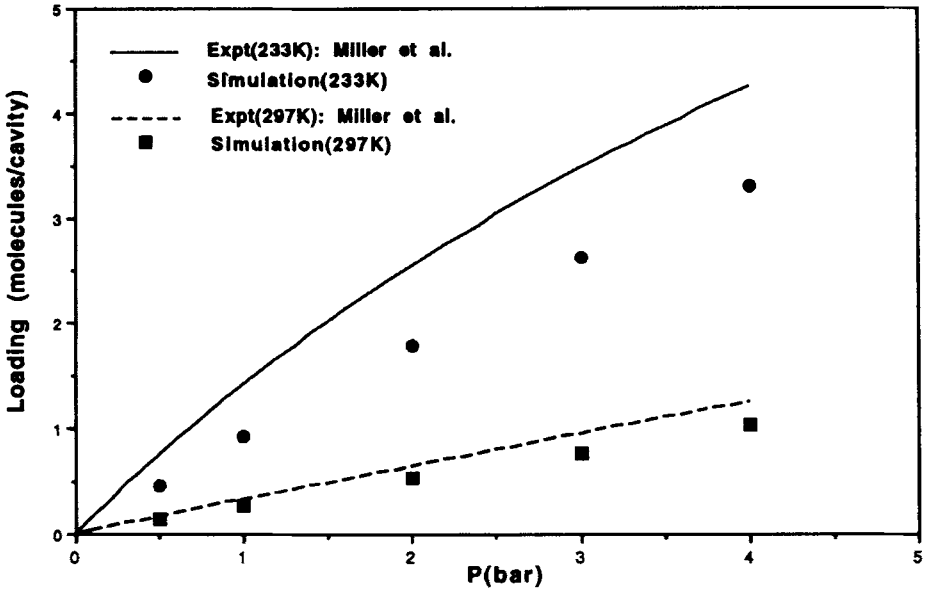

Figure 4 Adsorption isotherms for argon in 5A at 233 K and 297 K. Simulation results are compared to experimental results of Miller *et al.* [19].

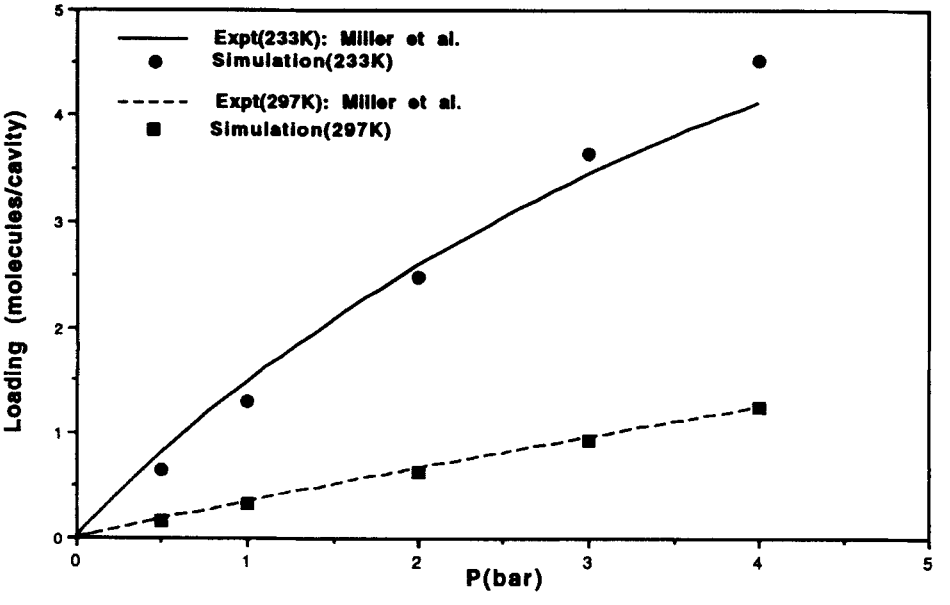

Figure 5 Adsorption isotherms for oxygen in 5A at 233 K and 297 K. Simulation results are compared to experimental results of Miller *et al.* [19].

Downloaded At: 19:23 14 January 2011

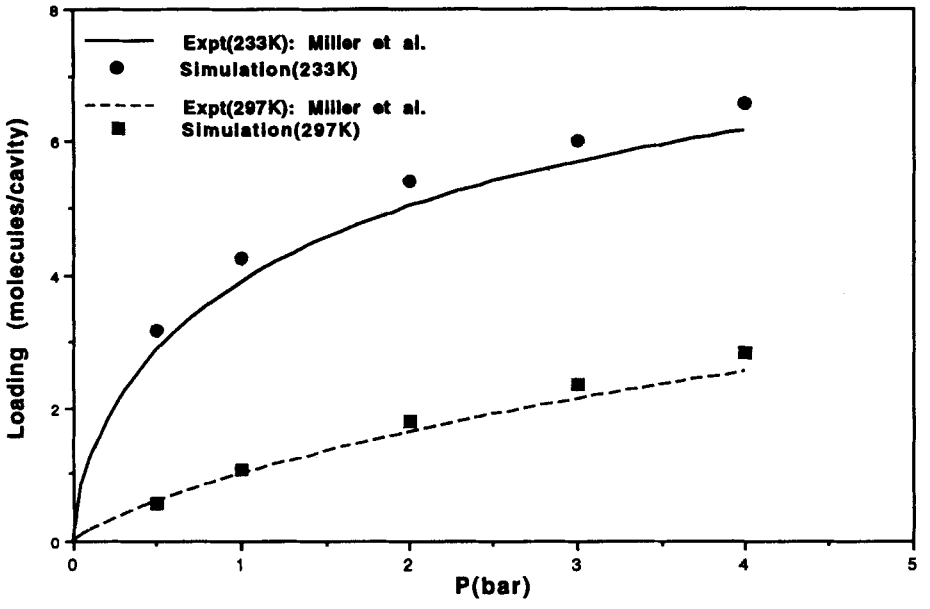

Figure 6 Adsorption isotherms for nitrogen in 5A at 233 K and 297 K. Simulation results are compared to experimental results of Miller *et al.* [19].

Downloaded At: 19:23 14 January 2011

consistently smaller than Miller's measurements. This suggests that the potential model used in the simulation underestimates the attractive interaction potential between argon and the 5A lattice. The enhancement of nitrogen adsorption over that of oxygen in 5A is reproduced well by the simulations, suggesting that the strength of the Coulombic interactions is represented with reasonable accuracy. Figures 7 and 8 show a comparison of simulation results with the experimental data of Miller [19] for argon/oxygen/nitrogen mixtures. In these figures, predicted and experimental loadings are plotted for oxygen and nitrogen as functions of partial pressures of the corresponding components. Simulation tends to predict loadings higher than those obtained experimentally, particularly at higher pressures. The relative selectivity of nitrogen over oxygen predicted by simulation was compared with experiment by calculating the N_2/O_2 separation factor α_{N-O} defined as,

$$\alpha_{N-O} = [X_{N_2}/X_{O_2}]/[Y_{N_2}/Y_{O_2}] \tag{15}$$

where X_i and Y_i are the molar fractions of component i in the adsorbed phase and in the gas phase, respectively. As can be seen in Figure 9, where α_{N-O} is shown as a function of Y_{N_2}, the N_2/O_2 selectivity predicted by simulation is in good agreement with experiment over a wide range of Y_{N_2}. Predictions by simulation for the N_2/O_2 selectivity were also tested against the experimental data of Huang [24] for the adsorption isotherm of binary mixtures of oxygen and nitrogen at 298 K and total pressure of 0.8 bar. Figure 10 compares the predicted and experimental values for X_{N_2} shown as a function of Y_{N_2}. Also shown in the figure is the comparison for the total amount of adsorbed oxygen and

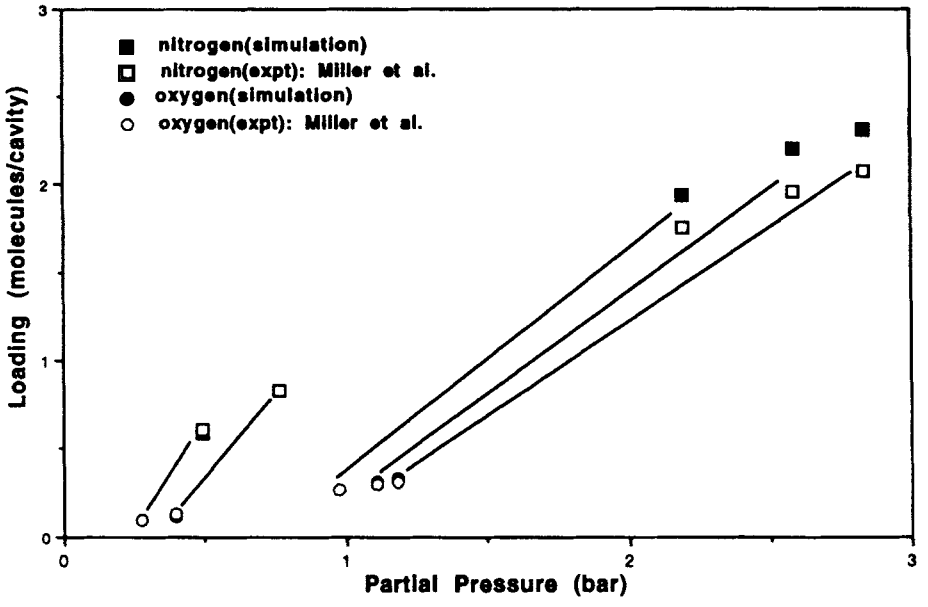

Figure 7 Adsorption of argon/oxygen/nitrogen mixtures in 5A at 297 K. Simulation results for oxygen and nitrogen loadings are compared to experimental results of Miller *et al.* [19]. The lines connect values obtained from a single simulation.

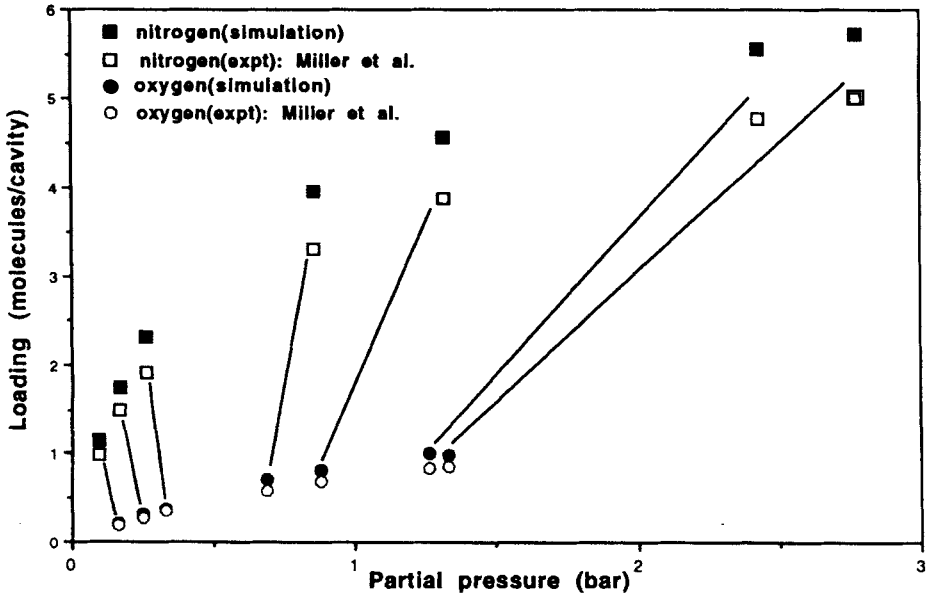

Figure 8 Adsorption of argon/oxygen/nitrogen mixtures in 5A at 233 K. Simulation results for oxygen and nitrogen loadings are compared to experimental results of Miller *et al.* [19]. The lines connect values obtained from a single simulation.

Downloaded At: 19:23 14 January 2011

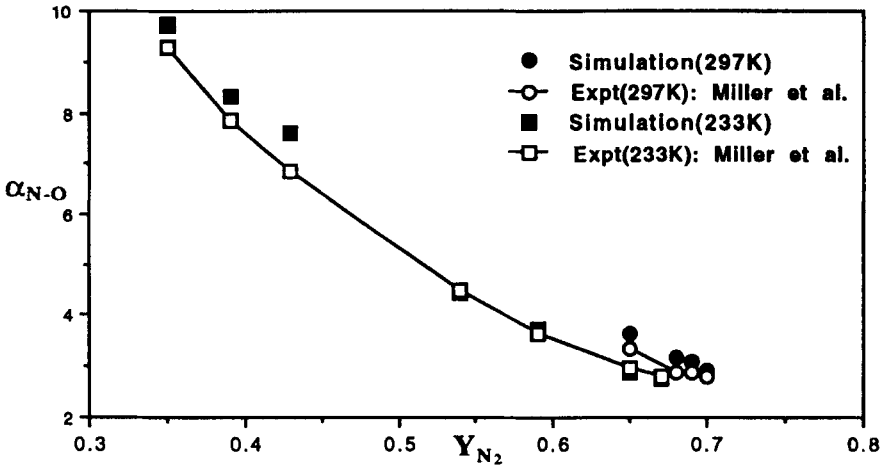

Figure 9 Adsorption of argon/oxygen/nitrogen mixtures in 5A at 233 K and 297 K. Simulation results for the N_2/O_2 separation factors are compared to experimental results of Miller *et al.* [19].

Downloaded At: 19:23 14 January 2011

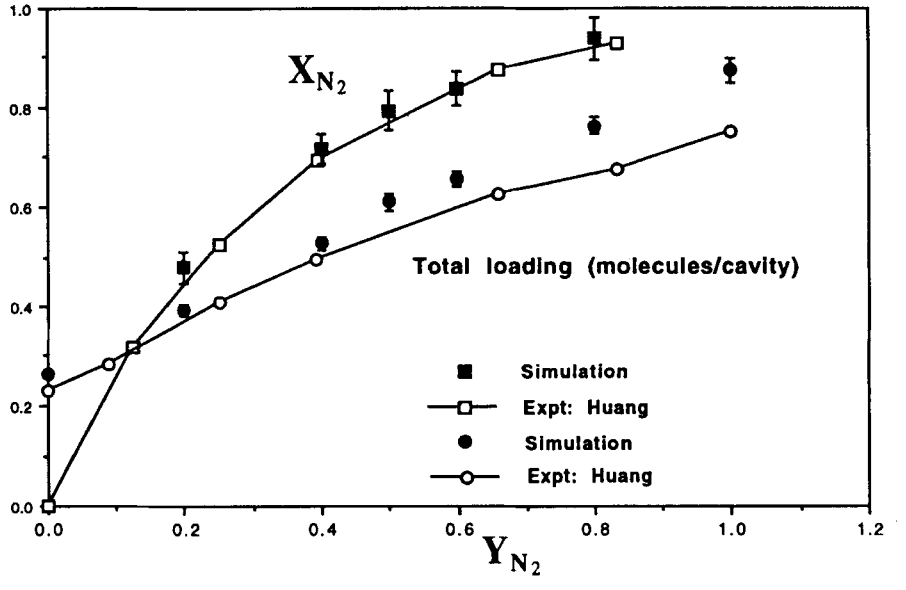

Figure 10 Adsorption of oxygen/nitrogen mixtures in 5A at 298 K and 0.8 bar. Simulation results for the molar fraction of nitrogen in the adsorbed phase and the total loading are compared to experimental results of Huang [23].

nitrogen. While the total loading is slightly overpredicted by simulation, the relative quantity α_{N-O} is clearly in good agreement with the experimental measurements.

Figure 11 shows the distributions of the single molecule adsorption energies, U_1, of argon, oxygen, and nitrogen in the 5A lattice obtained from the simulations performed at 297 K and 4.0 bar, where U_1 is the average potential energy of an adsorbate molecule

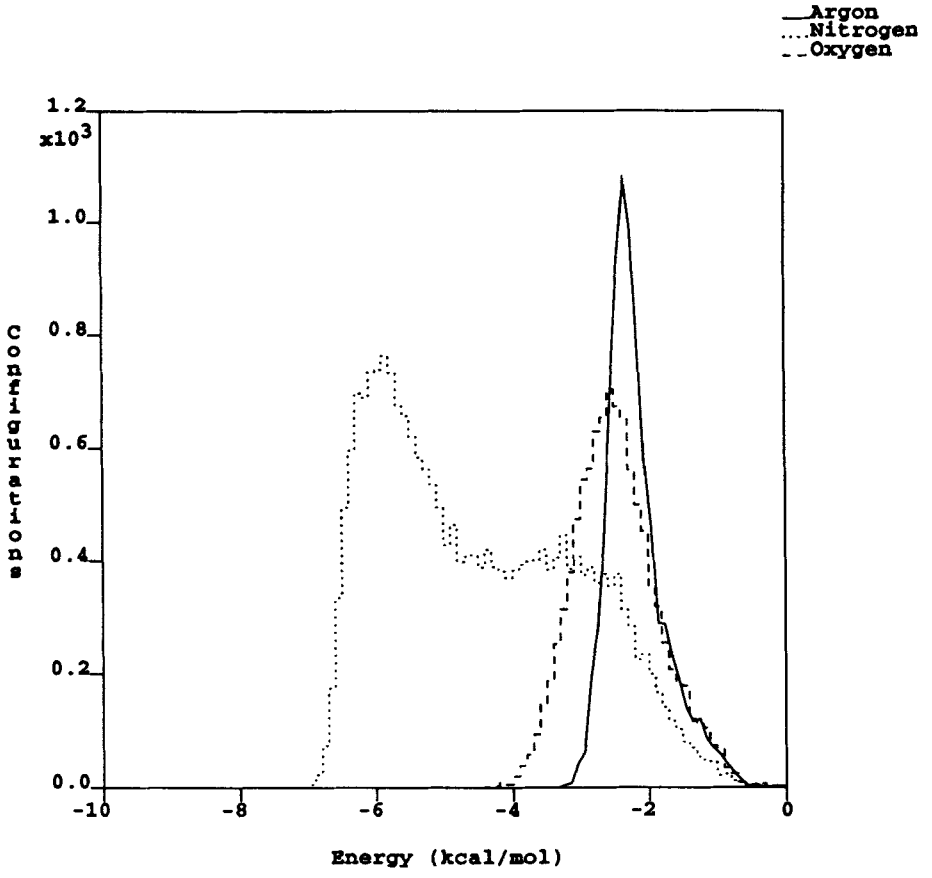

Figure 11 Simulation results for the distribution of single molecule potential energies, U_1, are shown for adsorption of argon, oxygen, and nitrogen in 5A. Simulations were performed at 297 K and 4 bar.

Downloaded At: 19:23 14 January 2011

interacting with the zeolite lattice and with other adsorbate molecules. It is evident that the binding of nitrogen is significantly stronger than that of argon or oxygen. Moreover, the binding of nitrogen in the 5A lattice is characterized by a bimodal distribution of the adsorption energies. Figure 12 shows the distribution of nitrogen adsorption sites within the zeolite lattice corresponding to the two distinct ranges of adsorption energies, Figure 12(a): $U_1 < 4.5$ kcal/mol and Figure 12(b): $U_1 > 4.5$ kcal/mol. The dots in these figures represent centres of masses of adsorbate positions generated by the simulations. It is clear from an examination of these three dimensional representations of the molecular distributions that the adsorption sites with lower binding energies are correlated to the locations of ions (shown as solid spheres) while those with higher binding energies are evenly distributed within the zeolite cavity. Figures 13 and 14 show the distributions of adsorption sites in 5A for argon and oxygen, respectively. The relatively uniform distributions of adsorbates within the zeolite cavities shown in these figures are clearly different from the more localized adsorption of nitrogen molecules. These observations suggest that the

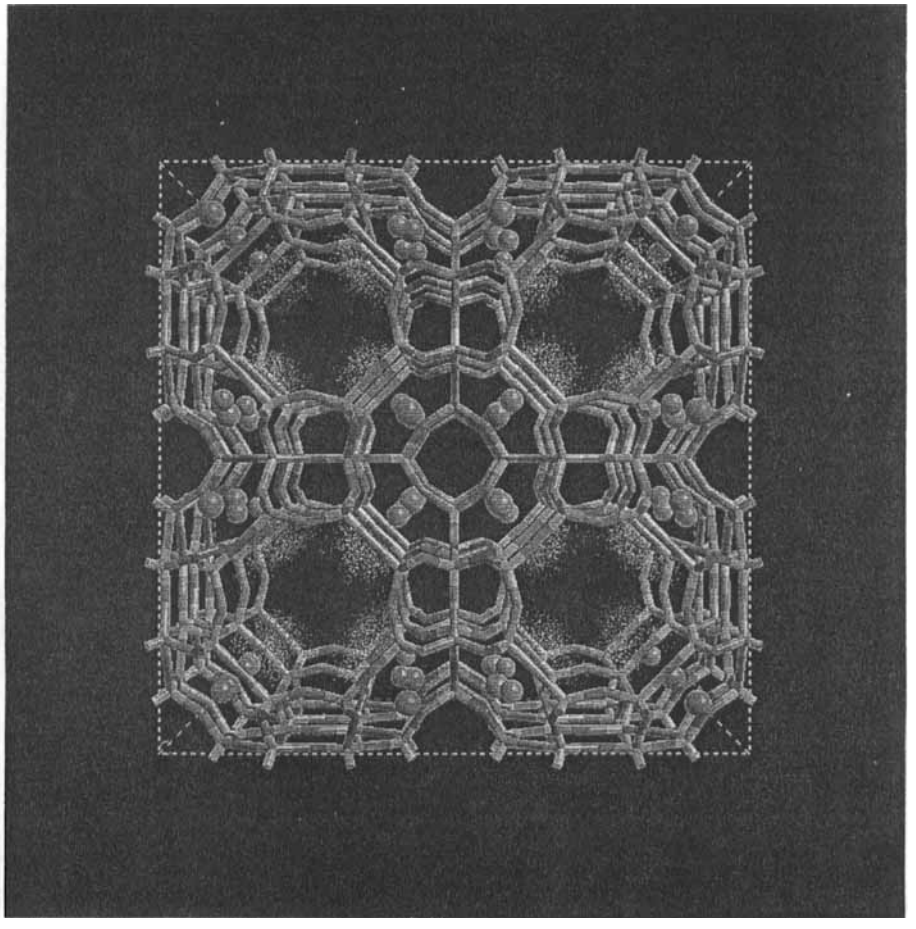

(a)

Figure 12 Simulation results for the distribution of nitrogen in 5A is shown for molecules with (a) $U_1 < -4.5$ kacl/mol and (b) $U_1 > -4.5$ kcal/mol. Simulation was performed at 297 K and 4 bar. See Color Plate I(a).

preferential adsorption of nitrogen in the 5A zeolite is largely due to the Coulombic interaction between the quadrupole moment of nitrogen molecule and the calcium ions.

4.1.2 Effects of calcium-sodium ion exchange Having established the reliability of the simulation results for the N_2/O_2 selectivity in 5A, we proceeded to apply the method to investigate the effect of the calcium-sodium ion exchange on the N_2/O_2 selectivity of zeolite type A. Additional simulations of N_2/O_2 binary mixtures at 298 K and 0.8 bar were performed with fully calcium exchanged and fully sodium exchanged forms of zeolite A (CaA and NaA, respectively). Lattices for CaA and NaA were constructed based on the structural parameters determined from x-ray diffraction measurements by Pluth and Smith [25, 26]. A cubic unit cell of CaA containing 8 large cavities is 24.44 Å in side length, and all calcium ions lie near the centres of 6-rings with approximately

Downloaded At: 19:23 14 January 2011

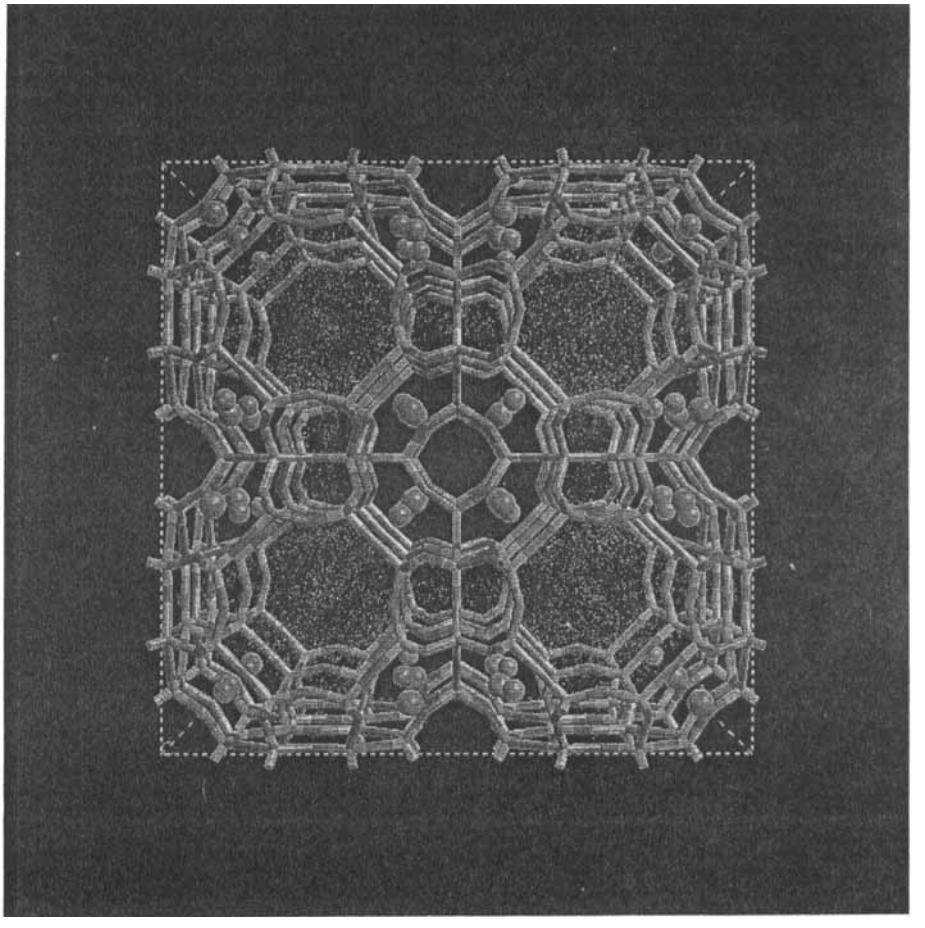

(b)

Figure 12 *(Continued)* See Color Plate I(b).

four-fifths of them projecting into the large cage and the remaining one-fifth projecting into the sodalite cage. Accordingly, a CaA lattice with unit cell composition $Ca_{48}Al_{96}Si_{96}O_{348}$ was prepared by placing 37 calcium atoms at the sites randomly from the cation sites in the large cages and the remaining 11 calcium atoms randomly at the cation sites in the sodalite cages, but excluding those sites which are adjacent to the occupied cation sites of the former type. A NaA lattice with unit cell composition $Na_{96}Al_{96}Si_{96}O_{348}$ and cell length 24.555 Å was prepared using the framework coordinates and the extra framework cation coordinates and occupancies given in reference [26]. Sodium atoms were placed in the lattice as follows: 64 near the centres of 6-rings, 24 in the planes of 8-rings, and 8 in the large cavities opposite to 4-rings. While the 6-ring and 8-ring sites are fully occupied, the occupancy of the 4-ring sites was chosen randomly to give the experimental 8.3% occupancy.

Figure 15 compares the simulation results for the N_2/O_2 selectivity obtained from simulations of N_2/O_2 binary mixtures in the CaA, NaA and 5A lattices. The figure

Downloaded At: 19:23 14 January 2011

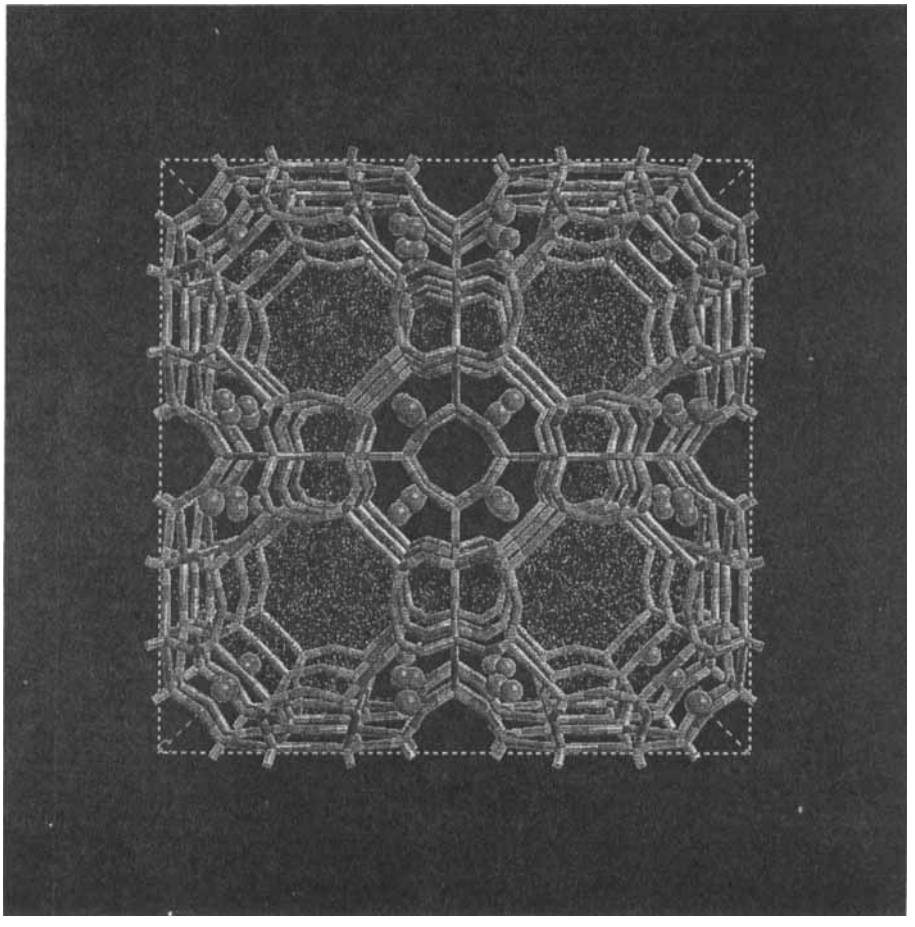

Figure 13 Simulation results for the distribution of argon in 5A is shown. Simulation was performed at 297K and 4 bar. See color plate I(c).

Downloaded At: 19:23 14 January 2011

shows the nitrogen molar fractions in the adsorbed phase as functions of that in the gas phase. Simulations predict that the N_2/O_2 selectivity is similar for CaA and NaA and that these forms of zeolite A are better separators of air than 5A. The simulations were carried out with a charge assignment of 1.61 |e| and 1.0 |e| for calcium and sodium, respectively, and the ordering of these type A zeolites with respect to N_2/O_2 selectivity is a consequence of the balance between the numbers, accessibility, and the charges of the cations. While there are 6 cations per cavity with charge 1.61 |e| in CaA, there are 12 cations with charge 1.0 |e| in NaA, and three of those are located on the planes of 8-membered rings which are more accessible than the calcium ions to the adsorbate molecules. This results in the prediction that CaA and NaA are comparable in N_2/O_2 selectivity. The 5A lattice with four each of the cations per cavity with charges 1.0 |e| and 1.61 |e| is predicted to be lower in N_2/O_2 selectivity than either of the fully exchanged forms. However, these findings are in conflict with experimental observations [27] that

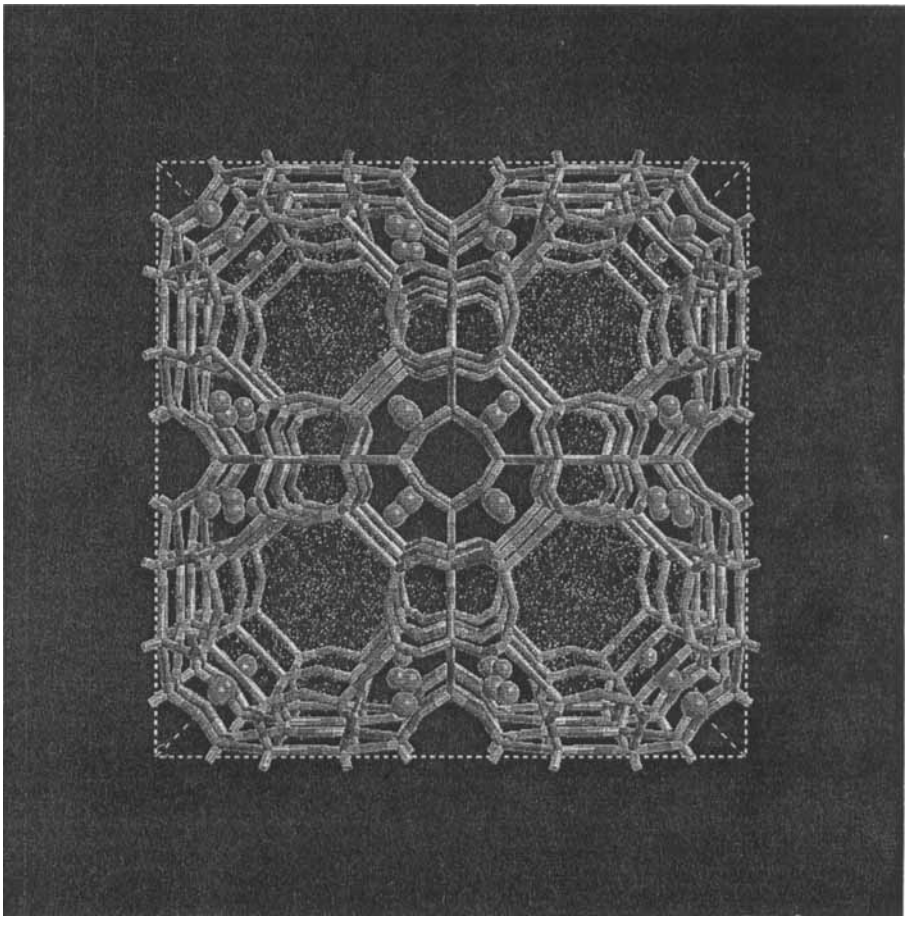

Figure 14 Simulation results for the distribution of oxygen in 5A is Shown. Simulation was performed at 297K and 4 bar. See color plate I(d).

Downloaded At: 19:23 14 January 2011

N_2/O_2 selectivity increases with an increase in the sodium to calcium ion exchange. This suggested to us that the relative magnitudes of the charges assigned to sodium and calcium may be in error.

Although the quantum mechanical calculations showed that there is negligible charge transfer to the sodium ion from the framework oxygen [21], a reexamination of the charge assignment for the sodium ion was warranted. Empirical determination of the effective charge on the sodium ion was carried out using a fitting procedure, which treats q_{Na} and $\varepsilon_{Oz(Al-O-Si)}$ as adjustable parameters while fixing all other ε_i at the values given in Table 2, to obtain consistency with experimental K_H values for oxygen and nitrogen in NaA. With the choice $q_{Na} = 0.92|e|$ and $\varepsilon_{Oz(Al-O-Si)} = 0.267$ kcal/mol, experimental K_H values [16] for oxygen and nitrogen at 298 K, 0.21 molecules/cavity/bar and 0.75 molecules/cavity/bar respectively, were reproduced. In order to

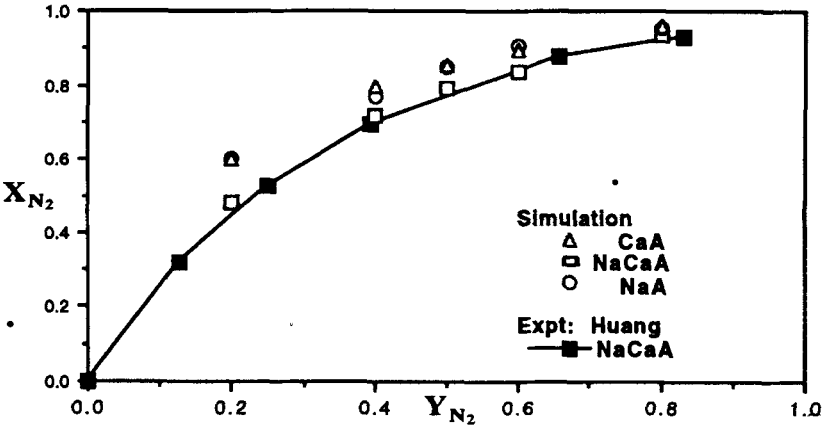

Figure 15 Adsorption of nitrogen/oxygen mixtures in CaA, NaA, and 5A at 298 K and 0.8 bar. Simulation results obtained using $q_{Na} = 1.0|e|$ and $q_{Ca} = 1.61\,|e|$ are compared to experimental results of Huang [24].

Downloaded At: 19:23 14 January 2011

maintain the previously obtained consistency with the experimental K_H values for 5A, a re-adjustment of q_{Ca} value was necessary to compensate for the reduction in the value of q_{Na}. Using ($q_{Na} = 0.92\,|e|$ and $q_{Ca} = 1.65\,|e|$) and ε_i values given in Table 2, Henry's constants for oxygen and nitrogen were evaluated at 0.33 molecules/cavity/bar and 1.35 molecules/cavity/bar at 298 K. These are in good agreement with experimental values (0.296 molecules/cavity/bar and 1.24 molecules/cavity/bar for oxygen and nitrogen, respectively) given in reference [16] and (0.344 molecules/cavity/bar and 1.44 molecules/cavity/bar for oxygen and nitrogen, respectively) given in reference [19]. Using the revised charge assignment ($q_{Na} = 0.92\,|e|$ and $q_{Ca} = 1.65\,|e|$) and the LJ potential parameters given in Table 2, the simulations of the N_2/O_2 binary mixtures at

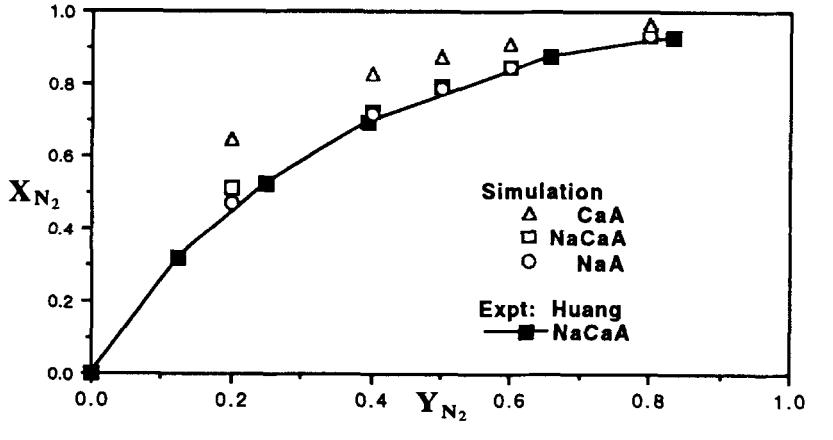

Figure 16 Adsorption of nitrogen/oxygen mixtures in CaA, NaA, and 5A at 298K and 0.8 bar. Simulation results obtained using $q_{Na} = 0.92|e|$ and $q_{Ca} = 1.65\,|e|$ are compared to experimental results of Huang [24].

298 K and 0.8 bar in the NaA, 5A, and CaA lattices were repeated. Figure 16 shows the result of the simulations. It can be seen that the N_2/O_2 selectivity determined with the revised charge assignment increases in the order NaA < 5A < CaA, as a result of a decrease for NaA and an increase for CaA of the N_2/O_2 selectivity compared to the result of the earlier calculations. The N_2/O_2 separation factors, α_{N-O}, for NaA, 5A, and CaA are in the ranges 3.6–3.8, 3.7–4.2, and 6.5–7.3, respectively. In summary, effective charges which are less than the values corresponding to full ionization are required for both sodium and calcium ions in order to fit experimental Henry's constants [16, 19] for oxygen and nitrogen in 5A and NaA and these lead to the prediction of increasing N_2/O_2 selectivity with Na to Ca exchange. The partial charges on the cations may be a consequence of charge transfer from framework oxygens. Alternatively, it may be attributed to hydroxylation of cations which can occur [27, 28] during thermal activation of zeolites. It is of interest, therefore, to predict the N_2/O_2 selectivity for the "ideal" case where the charges on the cations are $q_{Na} = 1.0|e|$ and $q_{Ca} = 2.0|e|$. This allows us to set upper limits to predicted N_2/O_2 selectivities. The results of such calculations are given in Figure 17, which shows that the N_2/O_2 selectivity is substantially increased for all three zeolites. The N_2/O_2 separation factors α_{N-O} are calculated to be in the range 5–6, 11–14, and 16–26 for NaA, 5A and CaA, respectively. The N_2/O_2 selectivity increases in the order NaA < 5A < CaA, as expected, but the consistency with experimental N_2/O_2 selectivity is lost.

Downloaded At: 19:23 14 January 2011

4.2 *Zeolite Types X and Y*

The effect of the calcium-sodium exchange and of the aluminium-silicon ratio on N_2/O_2 selectivity was investigated for zeolites with a faujasite framework by performing simulations of N_2/O_2 mixtures in CaX, NaX, and NaY. A cubic unit cell of CaX with

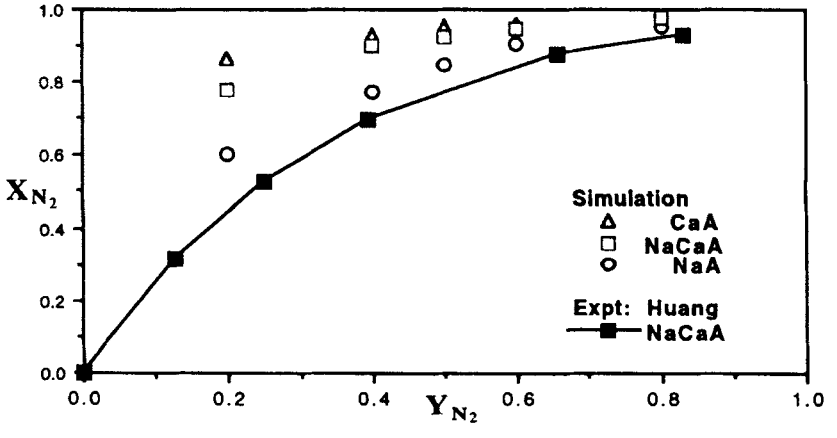

Figure 17 Adsorption of nitrogen/oxygen mixtures in CaA, NaA, and 5A at 298K and 0.8 bar. Simulation results obtained using $q_{Na} = 1.0|e|$ and $q_{Ca} = 2.0|e|$ are compared to experimental results of Huang [24].

formula $Ca_{43}Al_{86}Si_{106}O_{348}$ was constructed using the unit cell dimension (24.97 Å), the atomic coordinates, and the extra framework cation distribution determined by Pluth and Smith [29]. It has 13 calcium in type I sites, 5 in type I' sites, and 25 in type II sites. The 13 calcium were placed in type I sites which were chosen randomly from 16 sites of this type, the 5 calcium were placed in type I' sites which are not adjacent to the occupied type I sites, and finally the 25 calcium were placed in type II sites chosen randomly from 32 sites of the type. The sodium-exchanged from, NaX, with unit cell formula $Na_{86}Al_{86}Si_{106}O_{348}$ was constructed using the unit cell dimension (25.06 Å) and the fractional coordinates determined by Shepelev [30]. The sodium ions were distributed according to the rule proposed by Newsam [31]. Type I' and type II sites are fully occupied accounting for 64 sodium, and the remaining 22 sodium occupy type III sites chosen at random. A unit cell of NaY with formula $Na_{57}Al_{57}Si_{135}O_{348}$ was constructed using the unit cell dimension (24.85 Å), the fractional coordinates, and the extra framework cation distribution determined by Fitch [32]. Type II sites are fully occupied with 32 sodium and type I sites and type I' sites are both partially occupied with occupancies of 7 and 18 sodium, respectively, with an imposed restriction that a simultaneous occupancy of adjacent type I and type I' sites is avoided. In all three structures, aluminium atoms are distributed on the silicon/aluminium sites such that the Loewenstein's rule of Al-O-Al linkage avoidance is obeyed.

Figures 18, 19 and 20 show the simulation results for N_2/O_2 binary mixtures at 298 K and 0.8 bar. Figure 18 compares the molar fractions of nitrogen in the adsorbed phase obtained for CaX, NaX, and NaY using cation charges given by $q_{Na} = 1.0|e|$ and $q_{Ca} = 1.61\,|e|$ and the LJ potential parameters given in Table 2. It can be seen that the N_2/O_2 selectivity for the sodium exchanged form is larger than that for the calcium exchanged form. This is again in conflict with experimental observation [27] regarding the effect of the calcium-sodium exchange on the N_2/O_2 selectivity. Figure 19 shows the same comparison for simulations carried out using the revised charge assignment

Downloaded At: 19:23 14 January 2011

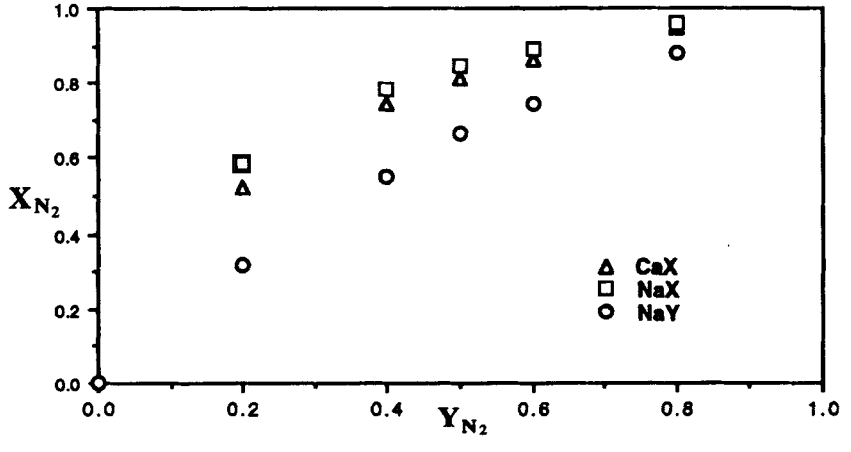

Figure 18 Adsorption of nitrogen/oxygen mixtures in CaX, NaX, and NaY at 298K and 0.8 bar. Simulation results obtained by using $q_{Na} = 1.0\,|e|$ and $q_{Ca} = 1.61\,|e|$ and 0.8 bar.

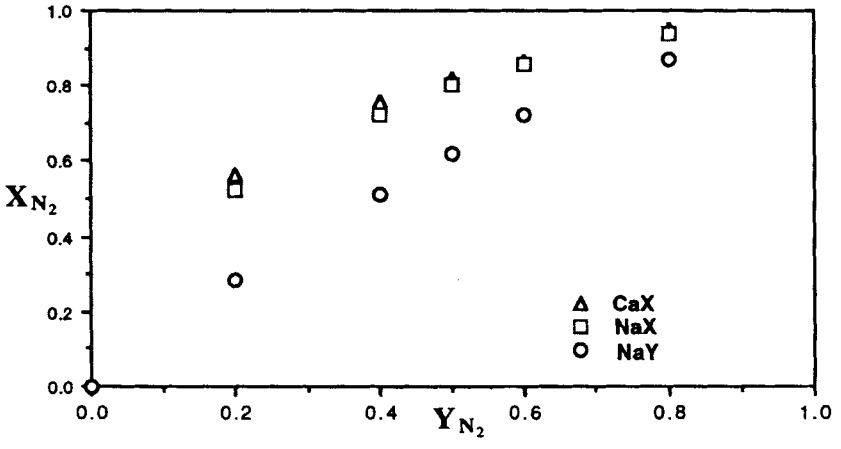

Figure 19 Adsorption of nitrogen/oxygen mixtures in CaX, NaX, and NaY at 298K and 0.8 bar. Simulation results obtained by using $q_{Na} = 0.92|e|$ and $q_{Ca} = 1.65|e|$ are shown.

Downloaded At: 19:23 14 January 2011

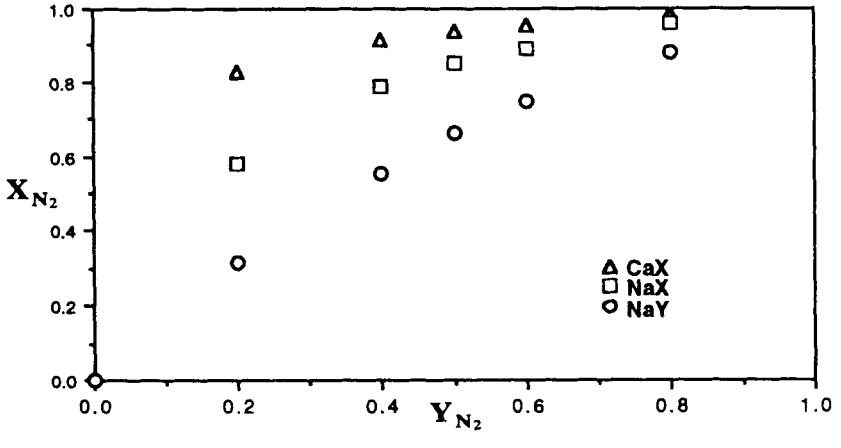

Figure 20 Adsorption of nitrogen/oxygen mixtures in CaX, NaX, and NaY at 298K and 0.8 bar. Simulation results obtained by using $q_{Na} = 1.0|e|$ and $q_{Ca} = 2.0|e|$ are shown.

$q_{Na} = 0.92|e|$ and $q_{Ca} = 1.65|e|$. With these charges the N_2/O_2 selectivity is predicted to be larger for CaX than for NaX in agreement with the experimental observations. As expected, the N_2/O_2 selectivity for NaY is smaller than that for NaX as a result of the reduced number of sodium ions required for the electric neutrality. Using the simulation results given in Figure 19, the N_2/O_2 separation factors, α_{N-O}, for CaX, NaX, and NaY are determined to be in the range 4.2–5.2, 3.9–4.4, and 1.6–1.7, respectively. Figure 20 shows the simulation results for the "ideal" case where the cations retain the formal charges, $q_{Na} = 1.0|e|$ and $q_{CA} = 2.0|e|$. As expected, the N_2/O_2 selectivity for CaX is increased substantially compared to the result obtained using fractional

charges. The N_2/O_2 separation factors calculated from the simulation results shown in Figure 20 are in the range 12.9–18.9, 5.4–6.0, and 1.8–2.0 for CaX, NaX, and NaY, respectively. The present simulation shows that the increase in the average value of α_{N-O} for CaX accompanying the change from the partial ionization (1.65 |e|) to full ionization (2.0 |e|) of the calcium is by a factor of 3.3. With formal charges used for sodium and calcium ions simulation results were such that the average value of the N_2/O_2 separation factors obtained for CaX is larger than that for NaX by the factor of 2.7, while with partial charges ($q_{Na} = 0.92$ |e| and $q_{Ca} = 1.65$ |e|) the N_2/O_2 separation factors obtained for CaX and NaX are comparable. For the oxygen/nitrogen mixture corresponding to the air composition, i.e. $Y_{N2} = 0.8$, α_{N-O} is calculated at 4.8 and 12.9 using $q_{Ca} = 1.65$ |e| and 2.0 |e|, respectively. It is notable that N_2/O_2 separation factor for air in CaX reported by Coe [28], 7.3 at 303K and atmospheric pressure, is bracketted by these values obtained by simulations. This suggests that the charge on the calcium ions in the CaX sample used in reference [28] is somewhere between 1.65 |e| and 2.0 |e|.

5. CONCLUSIONS

Downloaded At: 19:23 14 January 2011

Adsorbate-zeolite interaction potentials pertinent to the adsorption of air in zeolites were determined based on a semi-empirical approach using experimental values [16, 20] of Henry's constants for argon, oxygen, and nitrogen in silicalite, 5A and NaA. The present work has resulted in the dispersion interactions of adsorbate molecules with zeolite lattices which depend on zeolite type and extra framework cation types and in the assignment of partial charges to the extra framework cations whose effective charges may depend on framework type and on the conditions under which zeolite samples are activated. The LJ parameter for the zeolitic oxygen, ε_{Oz}, was determined as 0.202 kcal/mol for silicalite 0.334 kcal/mol for 5A, and 0.267 kcal/mol for NaA. The charges on the cations required to obtain reasonable agreement with experimental N_2/O_2 selectivities [16, 19, 24] in 5A and NaA were $q_{Na} = 0.92$ |e| and $q_{Ca} = 1.65$ |e|. The N_2/O_2 separation factors for air obtained for CaX by simulation using cation charges 1.65 |e| and 2.0 |e| bracket the experimental value obtained by Coe [28]. This suggests that the effective charge on calcium ions in the CaX sample used in reference [28] is in the range between 1.65 |e| and 2.0 |e|.

Simulation results for the N_2/O_2 selectivities of zeolites of type A and faujasite framework have been shown to be sensitive to the sizes of the charges assigned to extra framework cations. In the examination of the dependence of the N_2/O_2 selectivity on the extent of calcium-sodium ion exchange in zeolite types A and X, small changes (<0.1 |e|) in the charges assigned to sodium and calcium ions were shown to cause a reversal of the ordering of the selectivities with respect to the ion exchange. With fully ionized cations, simulation predicts that the N_2/O_2 selectivity of CaX is superior to that NaX, while comparable selectivities are predicted for the two forms of the zeolite with the partial ionization given by $q_{Na} = 0.92$ |e| and $q_{Ca} = 1.65$ |e|. This is consistent with the experimental findings by Coe [27] on the effect of the cation charges on N_2/O_2 selectivity which showed that the superior air separation of the calcium form of zeolite type X compared to the sodium form is manifested only with adsorbents in a fully dehydrated/dehydroxylated state.

Determination of adsorbate-zeolite interaction potentials based on the semi-empirical approach used in the present work is complicated by the dependence [22] of polarizabitity of zeolitic oxygens on the framework atom types and the extra framework cation types and by the dependence [27, 28] of effective charges of the extra framework cations on the conditions under which the zeolite samples are activated, which might explain the discrepancies between available experimental adsorption data. Further investigation of adsorbate-zeolite interactions using the semi-empirical approach of this work would require accurate measurements of adsorption properties made on zeolite samples prepared under carefully controlled conditions.

Acknowledgements

The authors would like to thank A. Chaffee for providing experimental adsorption isotherms for silicalite and F. Fitch, R. J-M. Pellenq, and S. J. Cook for useful discussions.

References

[1a] G. B. Woods and J. S. Rowlinson, "Computer simulations of fluids in zeolites X and Y", *J. Chem. Soc. Faraday Trans.* **85** (2), 765 (1989).
[1b] F. Karavias and A. L. Myers, "Monte Carlo simulations of adsorption of non-polar and polar molecules in zeolite X", *Mol. Simul.*, **8**, 23 (1991).
[1c] S. J. Goodbody, K. Watanabe, D. MacGowan, J. P. R. B. Walton and N. Quirke, "Molecular simulation of methane and butane in silicate", *J. Chem. Soc. Faraday Trans.*, **87**, 1951 (1991).
[1d] D. M. Razmus and C. K. Hall, "Prediction of gas adsorption in 5A zeolites using Monte Carlo simulation", *AIChE J.*, **37**, 769 (1991).
[1e] R. F. Cracknell and K. E. Gubbins, "Molecular simulation of adsorption and diffusion in VPI-5 and other aluminophosphates", *Langmuir*, **9**, 824 (1993).
[2] M. P. Allen and D. J. Tildesley, *Computer Simulation of Liquids*, Clarendon, Oxford, 1987.
[3] *The Problem of Long-Range Forces in the Computer Simulation of Condensed Media*, D. Ceperley, Ed., National Information Service, Springfield, 1980.
[4] T. L. Hill, *Statistical Mechanics*, McGraw-Hill Book Company Inc., New York, 1956.
[5] J. O. Hirschfelder, C. F. Curtiss and R. B. Bird, *Molecular Theory of Gases and Liquids*, Wiley, New York, 1954.
[6] D. E. Stogryn and A. P. Stogryn, "Molecular multipole moments", *Mol. Phys.*, **11**, 371 (1966).
[7] C. A. English and J. A. Venables, "Structure of the diatomic molecular solids", *Proc. R. Soc., London, Ser. A*, **340**, 57 (1974).
[8] C. S. Murthy, K. Singer, M. L. Klein and I. R. McDonald, "Pairwise additive effective potentials for nitrogen", *Mol. Phys.*, **41**, 1387 (1980).
[9] W. H. Press, B. P. Flannery, S. A. Teukolsky and W. T. Vetterling, *Numerical Recipes*, Cambridge University Press, Cambridge, 1986.
[10] K. A. van Genechten and W. J. Mortier, "Influence of the structure type on the intrinisic framework electronegativity and the charge distribution in zeolites with SiO_2 composition", *Zeolites*, **8**, 273 (1988).
[11] W. J. Mortier, S. K. Ghosh and S. Shankar, "Electronegativity equalization method for the calculation of atomic charges in molecules", *J. Am. Chem. Soc.*, **108**, 4315 (1986).
[12] V. M. Goldschmidt, *Geochemische Verteilungsgesetze der Elements*, Skrift Norske Vid. Akad., Oslo, (1926).
[13] K. Fajans and G. Joos, "Molrefraktion von ionen und molekulen im lichte der atomstruktur", *Z. Physik*, **23**, 1 (1924).
[14] K. Seff and D. P. Shoemaker, "The structures of zeolite sorption complexes. I. The structures of dehydrated zeolite 5A and its iodine sorption complex", *Acta Cryst.*, **22**, 162 (1967).
[15] H. van Koningsveld, H. van Bekkum and J. C. Jasen, "On the location and disorder of a tetrapropylammonium (TPA) ion in zeolite ZSM-5 with improved framework accuracy", *Acta Cryst.*, **B43**, 127 (1987).

Downloaded At: 19:23 14 January 2011

[16] D. H. Ruthven, "Sorption of oxygen, nitrogen, carbon monoxide, methane, and binary mixtures of these gases in 5A molecular sieve", *AIChE J.*, **22**, 753 (1976).
[17] G. A. Soriel, W. H. Granville and W. O. Daly, Adsorption equilibria for oxygen and nitrogen gas mixtures on 5A molecular sieves", *Chem. Eng. Sci.*, **38**, 1517 (1983).
[18] H. Verelst and G. V. Baron, "Adsorption of oxygen, nitrogen, and argon on 5A molecular sieve", *J. Chem. Eng. Data*, **30**, 66 (1985).
[19] G. W. Miller, K. S. Knaebel, and K. G. Ikels, "Equilibria of nitrogen, oxygen, argon and air in molecular sieve 5A", *AIChE J.*, **33**, 194 (1987).
[20] A. Chaffee, Private communication.
[21] J. Sauer and D. Deininger, "Interaction of ethene, 2-methylpropene and benzene with the Na^+ ion. II. Quantum chemical study of sorption complexes in faujasites", *Zeolites*, **2**, 114 (1982).
[22] R. J.-M. Pellenq and D. Nicholson, "In-framework ion dipole polarizabilities in non-porous and porous silicates and aluminosilicates, determined from Auger electron spectroscopy data", *J. Chem. Soc. Faraday Trans.*, **89**, 2499 (1993).
[23] Cerius^2 Computational Chemistry Software, Molecular Simulations Inc., Cambridge U.K. and Burlington MA, 1994.
[24] J. T. Huang, M. Sc. Thesis, Worcester Polytechnic Inst., 1970.
[25] J. J. Pluth and J. V. Smith, "Crystal structure of dehydrated Ca-exchanged zeolite A. Absence of near-zero-coordinate Ca^{2+}. Presence of Al complex", *J. Am. Chem. Soc.*, **105**, 1192 (1983).
[26] J. J. Pluth and J. V. Smith, "Accurate redetermination of crystal structure of dehydrated zeolite A. Absence of near zero coordination of sodium. Refinement of Si, Al-ordered superstructure", *J. Am. Chem. Soc.*, **102**, 4704 (1980).
[27] C. G. Coe and S. M. Kuznicki, "Polyvalent ion exchanged adsorbent for air separation", U. S. Patent 4 481 018 (1984).
[28] C. G. Coe, "Molecularly engineered adsorbents for air separation", in *Gas Separation Technology*, eds. E. F. Vansant and R. Dewolfs, p. 149, Elsevier Science Publishers B. V., Amsterdam, 1990.
[29] J. J. Pluth and J. V. Smith, "Positions of cations and molecules in zeolites with the faujasite-type framework. VII. Dehydrated Ca-exchanged X", *Mat. Res. Bull.*, **7**, 1311 (1972).
[30] Yu. F. Shepelev, A. A. Anderson and Yu. I. Smolin, "Sorbed molecules of benzene in the crystal structure of zeolite NaX", *Kristallografiya*, **33**, 359 (1988).
[31] J. M. Newsam, A. J. Jacobson and D. E. Vaughan, "Time-of-flight powder neutron diffraction studies of dehydrated synthetic gallosilicate zeolites X, XY, and Y", *J. Phys. Chem.*, **90**, 6858 (1986).
[32] A. N. Fitch, H. Jobic and A. Renouprez, "Localization of benzene in sodium-Y zeolite by powder neutron diffraction", *J. Phys. Chem.*, **90**, 1311 (1986).

Downloaded At: 19:23 14 January 2011